

Effect of Ceramic Reinforcement Chemistry on the Microstructure and Properties of Friction Stir Processed AA5083 - Al₂O₃ & WC & Si₃N₄ Composites

Saravanakumar, S.¹, Satheesh Kumar, S.², Chandrasekaran, M.³, Dadapeer, Doddamani.⁴,
Mohammed Musthaq, M. S.⁵ and Prakash, K. B.^{3*}

¹Department of Mechanical Engineering, M.Kumarasamy College of Engineering, Thalavapalayam, Karur, 639113, Tamil Nadu, India

²Department of Aeronautical Engineering, Nehru Institute of Technology, Coimbatore – 641105, Tamil Nadu, India

³Department of Mechanical Engineering, Bannari Amman Institute of Technology, Sathyamangalam, Erode-638401, Tamil Nadu, India

⁴Engineering Department, Mechanical and Chemical Unit, University of Technology and Applied Sciences Muscat, Sultanate of Oman

⁵Department of Mechanical Engineering, Al Ameen Engineering College, Erode-638104, Tamil Nadu, India

*Corresponding author (e-mail: kbprakash404@gmail.com)

Metal Matrix Composite (MMC) is a designed blend of a minimum of two constituents, i.e., matrix and reinforcement to achieve improved properties. A material with mechanical parameters intermediate between those of the matrix alloy and the ceramic reinforcement is produced by adding reinforced particles with high strength and modulus to a metal matrix. Aluminium metal matrix composites are incredibly strong and resistant to wear and fatigue. They are excellent structural materials for automotive and aeronautical applications because of their qualities. A new technique called friction stir processing (FSP) was developed from friction stir welding, which uses a tool to form a hole or groove in the matrix material with scattered reinforcing particles. This experiment provides information on the AA 5083 matrix material will be further reinforced will add (50% WC & Al₂O₃), (50% Al₂O₃ & Si₃N₄), (33.33% WC & Al₂O₃ & Si₃N₄) various ceramics in every specimen manufactured through FSP process. The mechanical behaviors (Hardness, Tensile) and tribological behavior such as wear analysis will be examined through Pin-On-Disc. Optical behavior analysis of the individual reinforcements will be evaluated through SEM analysis.

Keywords: FSP; silicon nitride; hardness test; tensile test; FESEM

Received: January 2025; Accepted: May 2025

The need for lightweight materials with increased mechanical properties prompted extensive research of metal matrix composite (MMC), which blends metal's good property with the finer property of strengthening phases [1]. Aluminum alloy, with the advantage of weight reduction, anti-corrosiveness, and moderate mechanical properties, has emerged as a favored potential candidate for broad engineering applications involving aerospace, vehicle, and ocean industries [2]. Among these alloys, AA5083 stands out as a high-strength, corrosion-resistant material, particularly in marine environments. Although aluminum has been commercially available for just over 100 years, it is now the second most widely used metal after steel in terms of both global production and expenditure, and it is undoubtedly the most significant nonferrous metal [3-5]. Aluminium is essential to almost every industry of the global economy, including consumer goods and mechanical equipment [6]. To improve the mechanical properties of AA5083, the incorporation of ceramic reinforcements such as Al₂O₃ (alumina), WC (tungsten

carbide), and Si₃N₄ (silicon nitride) into the alloy has garnered considerable attention. These reinforcements contribute significantly to enhancing the strength, wear resistance, and thermal stability of the composite. However, the fabrication of such composite materials requires effective processing methods to achieve uniform dispersion of the reinforcement phases and optimize their interaction with the matrix [7]. Some of the distinct and desirable characteristics are responsible for aluminum's engineering importance, including its high workability, corrosion resistance, light weight, and good electrical and thermal conductivity. Aluminium weighs roughly one-third as much as steel for the same volume, with a specific gravity of 2.7 compared to 7.85 for steel [8]. Although aluminum is seemingly at a disadvantage if being compared on a cost-per-pound basis, more appropriate comparison in some instances would be done on the basis of cost per unit volume. Friction Stir Processing (FSP) is a novel solid-state process capable of being employed for

metal matrix composite fabrication [9]. FSP, a variation of the widely known Friction Stir Welding (FSW), enables local property modification of materials through the intense plastic deformation generated. It therefore results in the matrix's reinforcing particles being distributed uniformly. The technique has clear benefits, including being able to work with high-strength alloys without melting, reducing defects, and improving the material's overall performance [10]. For example, a pound of aluminum can be used to make three times as many pieces of the same size as one pound of steel, which significantly reduces the cost difference and results in a homogeneous distribution of the matrix's reinforcing particles [11]. However, from an engineering perspective, aluminum's comparatively low modulus of elasticity—roughly one-third that of steel—is its most important drawback. This suggests that an aluminium component will deflect three times as much as a steel component of the same design under the same stress circumstances. It is usually necessary to improve stiffness by design modifications, such as the inclusion of ribs or corrugations, because alloying or heat treatment cannot significantly raise the modulus of elasticity [12].

Metal matrix composites (MMCs) research has garnered a lot of attention owing to their enhanced mechanical properties, which qualify them for use in diverse engineering applications. Several researchers have researched the reinforcement of aluminum alloys, particularly AA5083, with various ceramic particulates to improve their characteristics. In recent research, the mechanical behavior of AA5083, which has been reinforced using various reinforcements like Al₂O₃, WC, and Si₃N₄, has been researched. Mohsen Soori et al. [13] discussed the use of Friction Stir Processing (FSP) on different aluminum alloys like 6061, 5052, and 7075. They reported that FSP ideas are suggested as possible ways to develop FSP applications in manufacturing. Adem Kurt et al. [14] examined the addition of SiC (silicon carbide) particles into pure aluminum through FSP. They investigated the effect of various tool rotational and traverse speed, with and without the incorporation of SiC powders, on the surface microstructure of the modified surfaces. The surface modifications were observed using optical microscopy, and the mechanical properties of hardness and strength were measured. Their results indicated that improved distributions of SiC particles were obtained at higher rotational and traverse velocities. Furthermore, the surface composite made by FSP was also discovered to have three times greater hardness compared to the base aluminum. V. Jeganathan Arulmoni et al. [15] reported that when the tool depth was too great, it resulted in displacing the shoulder from the pre-placed SiC particles, preventing the generation of a surface composite. But when a target depth of 2.03 mm was applied, SiC particles were effectively introduced into the aluminum matrix. The surface

composite layer formed had good bonding with the aluminum substrate and no visible defects. Furthermore, a multi-axis computer-controlled machine with a feedback loop might be used to adjust the tool-spindle angle to match the surface curvature. The effects of friction stir processing and the number of passes on the electron beam additively generated Al-silicon alloy A04130 and Al-magnesium alloy AA5056 were examined by Tatiana Kalashnikova et al. [16]. For sheet AA5056 and cast A04130, the metal hardening exceeded typical levels without appreciably reducing ductility. The biggest improvement in mechanical characteristics was shown in AA5056, where tensile strength significantly improved. The mechanical characteristics and microstructural development of the friction stir-processed (FSP) hypereutectic aluminium alloy A390 were examined by Kamran Babapour Golafshani et al. [17]. Shear punch testing at various shear strain rates was used to determine the strain rate sensitivity of the FSP samples. Their findings revealed that the strain rate sensitivity index rose from 0.015 to 0.120 following three FSP passes, indicating improved mechanical properties upon processing. Use of Mesanja S et al. [18] used FSP to produce titanium carbide (TiC) particle-reinforced aluminum composites, demonstrated that processing conditions were important for TiC particle distribution and subsequently influenced the wear strength of processed composites. Mounarik Mondal et al. [19] examined how the aluminium 1060 matrix's mechanical qualities may be improved by integrating additive manufacturing (AM) and Friction Stir Processing (FSP). Ibrahim H. Zainelabdeen et al. [20] investigated the application of a pinless tool to alter the surface characteristics of Al 6061-O using a specifically made shoulder. Britto Joseph et al. [21] investigated the influence of adding alumina (Al₂O₃) particles to the 6063 aluminum alloy, which remarkably enhanced its mechanical properties. The ceramic particles were distributed on the alloy surface by the FSP method. Microhardness tests revealed that FSP-processed surface composites possessed a strength about 1.7 times higher than that of the untreated surfaces. J. Iwaszko et al. [22] found that FSP efficiently removed the inhomogeneous distribution and agglomeration of SiC particles that occurred in the as-cast composite. Processing resulted in homogenization of the material in the mixing zone and fragmentation of the composite matrix and SiC particles. Aluminum alloys are mainly classified into two broad groups according to their manufacturing process: wrought alloys and cast alloys. Low yield strength, strong ductility, high fracture resistance, and good strain hardening are among the advantageous forming qualities of wrought alloys, which are made via plastic deformation in the solid state [23]. Low melting points, great fluidity, and advantageous as-solidified structures and attributes are characteristics that set cast alloys apart. Because of these distinctions,

wrought and cast aluminium alloys fall into different groups.

This paper presents a detailed investigation of the mechanical behavior of AA5083 reinforced with Al₂O₃, WC, and Si₃N₄ particulates, fabricated by FSP. The study aims to evaluate the microstructure, hardness, tensile strength, wear resistance, and fracture behavior of the developed composite layers, providing a thorough comprehension of these composite materials' potential for challenging applications. Furthermore, the impact of various reinforcing types on the composite layers' mechanical performance will be examined, emphasizing the benefits and difficulties of using the FSP process to create such cutting-edge composite materials.

MATERIALS AND METHODS

Tungsten carbide is a type of ceramic material with a significantly higher melting temperature compared to many metals, making it particularly valuable for applications requiring exceptional performance under extreme conditions. Its high melting point, combined with its remarkable physical properties, makes tungsten carbide an ideal material for precision engineering, especially in areas where durability and resistance to harsh environments are essential. Tungsten carbide is highly regarded for its superior hardness, and outstanding wear resistance, making it a preferred material in industries such as manufacturing, mining, and aerospace. Additionally, tungsten carbide exhibits high thermal conductivity, which allows it to efficiently dissipate heat, further enhancing its performance in high-temperature applications. Tungsten carbide typically has a lower wear coefficient k , resulting in significantly reduced wear rates compared to steel, especially under harsh conditions. In the field of technical ceramics, alumina, also referred to as aluminium oxide, is one of the most commonly used and reasonably priced materials. The ceramic is made from raw materials that are both readily available and reasonably priced, making it an excellent choice in terms of cost efficiency when fabricated into various alumina shapes. Despite this, its overall durability and wide range of desirable properties make alumina a crucial material in fields such as aerospace, electronics, automotive, and chemical processing as shown in Table 2. The most thermodynamically stable form of silicon nitride, which is a chemical compound made up of silicon and nitrogen, is Si₃N₄. Due to this stability, Si₃N₄ is the most commercially significant and widely referred to when the term "silicon nitride" is used. As with other refractory materials, the precise characteristics and phases of silicon nitride depend heavily on these conditions shown in Table-3.

An AA5083 plate of 100 mm in length, 100 mm in width, and 10 mm in thickness was the material employed in this investigation. The reinforcements selected for the surface composites were R1 (WC + Al₂O₃), R2 (Al₂O₃ + Si₃N₄), and R3 (WC + Al₂O₃ + Si₃N₄). The common processing parameters for all reinforcement combinations included a tool rotation speed of 1000 rpm, a transverse speed of 20 mm/min, and an axial load of 10 kN. A non-consumable tool with a cylindrical pin diameter of 6 mm and a pin length of 2.7 mm was employed. It was constructed of high-carbon, high-chromium steel. The tool material's hardness value was 53 HRC. These parameters were applied consistently for the processing of the surface composites with different reinforcement combinations in Table 4.

Pure aluminum is used in casting due to its low melting temperature, which causes significant shrinkage and makes it prone to hot cracking, leading to high scrap rates. However, by adding small amounts of alloying elements, aluminum can acquire ideal casting characteristics, with increased strength [24]. Based on the basic concepts of FSW, FSP was developed as a general procedure for microstructural change [25]. Heat produced by the spinning tool's contact with the workpiece causes the material to deform below its melting point. A fine-grained, dynamically recrystallized microstructure is produced in the treated area as a result of significant plastic deformation brought on by the tool's pin's mechanical stirring action. Figure 1 shows a schematic representation of the FSP procedure. A detailed schematic of the FSP procedure is shown in Figure 1.a. & b. In FSP, a spinning tool that has been particularly made is inserted into a predetermined area of the plate. The tool features a concentric, larger-diameter shoulder and a small-diameter pin. When inserted, the rotating pin touches the surface and produces heat by friction, quickly softening a short column of metal. The shoulder regulates the depth of penetration and produces more frictional heat, which further softens a larger cylindrical area of metal [26]. Because of the tool pin, the shoulder's motion creates a forging force that limits the flow of metal. During FSP, the tool and workpiece reciprocate with respect to one another so that the tool moves over the region with overlapping passes, processing the entire zone to produce a fine-grain structure. The rotating tool plastically deforms the metal without melting, hence cooling the processed zone without solidification. Thus, a recrystallized, defect-free fine-grain microstructure is produced [27].

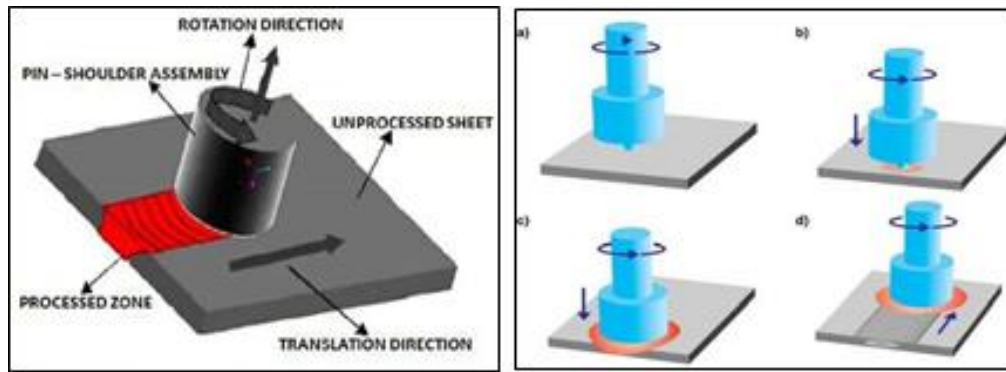


Figure 1(a) Friction Stir Processing **1(b)** Schematic illustration of FSP.

The die descends down to the shoulder touching the surface. The heat is generated mostly by the resistance between the workpiece and the shoulder. In order to control the heating and material flow, the relative pin and shoulder sizes are essential. The shoulder also serves to hold the heated material [28-29]. Rotating and stirring the material to get a homogenous microstructure and characteristics is the tool's second use. The tool's traverse speed (S) and rotating speed (N) are two important FSP parameters. Faster rotational speeds cause higher temperatures from higher frictional heating, creating more vigorous stirring and mixing of the material. But heating is not proportional to rotational speed since the friction factor between the tool face and workpiece changes with speed. Also, spindle tilt angle has a critical influence in the process. An appropriate tilt angle allows the tool shoulder to grip and shift the stirred material effectively, conveying the material from the pin face to the end. Outside the Thermo-Mechanical Affected Zone (TMAZ), there is the Heat Affected Zone (HAZ). This zone is subjected to thermal cycling but not plastic deformation. In heat-treatable aluminum alloys, the HAZ is a region where the temperature exceeds 250°C. This region's grain structure is identical to that of the parent material; however temperature exposure can significantly alter the precipitate structure [30-31].

This tool creates frictional heat and causes mechanical mixing the region it covers. One of the newest uses of FSP is the production of Surface Metal Matrix Composites (SMMCs). The frictional heat and stirring effect of the FSP tool aid the dispersal of

ceramic particles as reinforcements on the outer layer of light metals like magnesium and aluminium [32]. This chapter presents a detailed discussion on the selection of matrix and reinforcement materials, FSP tool design, and the identification of optimal processing parameters for developing composites using hybrid surfaces. It investigates the key factors in process optimization to obtain the required developing composites using hybrid surfaces mechanical properties and microstructure, exemplifying the versatility and efficiency of FSP fabricating surface composites [33-34]. The choice of material is a fundamental aspect in the composites' fabrication because it will directly influence the product's performance and cost. The ideal material is one that satisfies the demands of the application while keeping costs to a bare minimum. Various considerations have to be made in the choice of material, including whether it is readily available, whether it is compatible with the particular service conditions, and how easy it is to maintain during its life. The most important properties governing the material's appropriateness are its physical, chemical, and mechanical properties, which in sum will affect the material's performance, durability, and long-term stability of the material in the desired application. This tool pin design is responsible for the general efficiency of the FSP process since it facilitates significant plastic deformation in the base material, leading to improved mechanical properties in processed area. The use of aluminum alloy as the BM, combined with the threaded profile tool pin, was integral to achieving the desired outcomes in the FSP process, making it an essential aspect of this study cylindrical tool pin profile as shown in Figure 2.



Figure 2. Cylindrical Tool Pin Profile.

Table 1. Comparison of Properties of Tungsten Carbide vs. Steel.

Property	Tungsten Carbide	Steel
Hardness (Rockwell C)	70-80 HRC	50-60 HRC
Young's Modulus (GPa)	530-700	210-230
Density (g/cm ³)	15.6	7.85
Melting Point (°C)	2870	1370
Thermal Conductivity (W/m·K)	150-170	50-60
Wear Resistance (compared to steel)	100 times higher	-
Compressive Strength (MPa)	7000	2000

Table 2. Comparison of Properties of Alumina vs. Steel.

Property	Alumina	Steel
Hardness (Vickers)	2000-2500 HV	200-300 HV
Young's Modulus (GPa)	380-400	210-230
Density (g/cm ³)	3.95-4.05	7.85
Melting Point (°C)	1925	1370
Thermal Conductivity (W/m·K)	20-30	50-60
Wear Resistance (compared to steel)	10-50 times higher	-
Compressive Strength (MPa)	3500-4000	2000

Table 3. Comparison of Properties of Si₃N₄ vs. Steel.

Property	Silicon Nitride (Si ₃ N ₄)	Steel
Hardness (Vickers)	1800-2500 HV	200-300 HV
Young's Modulus (GPa)	300-350	210-230
Density (g/cm ³)	3.1-3.3	7.85
Melting Point (°C)	1900-2200	1370
Thermal Conductivity (W/m·K)	30-40	50-60
Wear Resistance (compared to steel)	10-20 times higher	-
Compressive Strength (MPa)	3000-4000	2000

Table 4. Name & Depth of Reinforcement Filled.

Sample	AA5083	WC	Al ₂ O ₃	Si ₃ N ₄
T1	AA5083	50%	50%	-
T2	AA5083	-	50%	50%
T3	AA5083	33.3%	33.3%	33.3%

RESULTS AND DISCUSSION

Table 5 details the levels and range of FSW process parameters employed in this research. Experimental setup has four main parameters, namely, SPEED (rpm), AXFC (KN), TOOL-TR (mm/min), and Reinforcements. SPEED (RPM), i.e., tool rotating speed, is set to the same level in all experiments as 1000 rpm achieve similarity in the process of welding. The transverse tool speed, is kept constant at a rate of 20 mm/min to ensure the tool travels at a constant speed along the material throughout the welding. Likewise, the AXFC (KN), or axial force exerted during the process, is kept constant at 10 kN across all trials to maintain the applied load on the workpiece consistent. The last parameter, Reinforcements, specifies the reinforcement materials that are incorporated into the base aluminum alloy. Three reinforcement combinations were utilized: WC+Al₂O₃ (tungsten carbide and alumina), Al₂O₃+Si₃N₄ (alumina and silicon nitride), and WC+Al₂O₃+Si₃N₄ (a combination of tungsten carbide, alumina, and silicon nitride). These parameters were judiciously chosen to explore how different reinforcing materials affect the functionality and calibre of welded joints in the FSW process with regard to factors like mechanical properties, microstructure, and general weld integrity.

The numbers given above give a vivid graphical illustration of the various stages in the process of grooving of the AA5083 test plate during Friction Stir Processing (FSP). Figure 3a depicts the AA5083 test plate prior to the grooving process, showing the material in its unchanged, Original state. This is the base image, representing the smooth, even surface of the plate before anything is changed. The plate, now, is ready for grooving, as required for the next steps in the FSP process.

Figure 3b shows the process when the AA5083 test plate is grooved. The tool, at this stage, starts cutting grooves in the material. The grooves are necessary for the reinforcements to be added in the next step, in an effort to enhance the material's qualities. The image depicts the interaction between the material and the tool, showing how the latter gradually removes material to form the required grooves. This is an important step as it illustrates the action of the tool on the plate surface and the creation of grooves that are essential for the improvement of the material. Lastly, Figure 3c illustrates the test plate once the process of grooving has been carried out. By this point, the grooves are complete, and the test plate is prepared to receive the reinforcement materials. The grooves, as can be seen from the image and identified as clear, produce cavities that provide a space to embed reinforcements to strengthening mechanical properties of the AA5083 plate using the FSP technique. Combined, these photographs 5 present a sequential and comprehensive picture of how the AA5083 test plate evolves from its original smooth surface to the grooved structure necessary for the subsequent stage of the FSP process. These photos are intended to demonstrate the significance of the grooving process in conditioning the material for reinforcement and enhancing its overall performance through Friction Stir Processing. Tensile strength was found by using a UTM machine on 50% WC + 50% Al₂O₃ test plates. The result indicated the maximum tensile strength is 185 N/mm². Vickers hardness testing machine is utilized for determining the hardness of friction stir treated area and shown in figure 4. The combined particles of 50% WC + 50% Al₂O₃ test plates had a maximum hardness of 132 HV-5, according to the evaluation.

Table 5. Levels and ranges of FSW process parameters.

S.no	Speed (rpm)	Tool-traverse Speed (mm/min)	Axial Force (kN)	Reinforcements
1	1000	20	10	WC+Al ₂ O ₃
2	1000	20	10	Al ₂ O ₃ +Si ₃ N ₄
3	1000	20	10	WC+Al ₂ O ₃ +Si ₃ N ₄

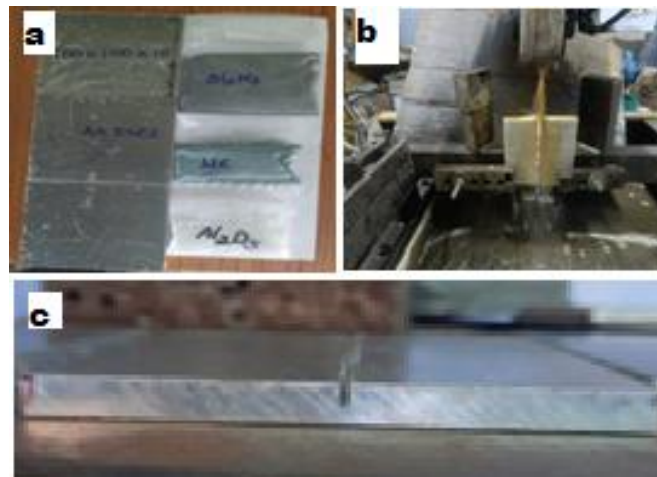


Figure 3(a) Before grooving, (b) During grooving, (c) After grooving of AA 5083 test plate

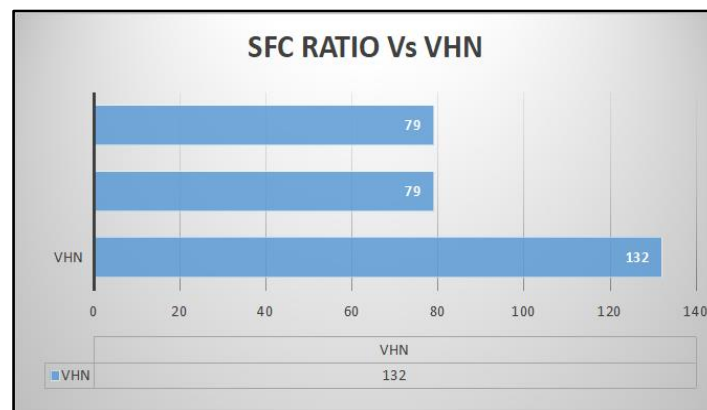


Figure 4. Hardness Results of Surface Composite.

Wear test was analyzed based on the Pin-on-Disc test, which is used to measure wear loss under a standard test condition. In this situation, test conditions were set constant with 20 N load, 500 seconds test duration, 40 mm pin diameter, and 478 RPM speed. The test specimen weight was determined before and after the wear test to find wear loss. The samples included various reinforcement combinations such as WC+Al₂O₃, Al₂O₃+Si₃N₄, and WC+Al₂O₃+Si₃N₄. Following the wear test, the initial and final weights demonstrated the following data: for WC+Al₂O₃ sample, the initial weight was 1.305 g and after the test the weight was 1.298 g, thereby a wear loss of 0.007 g. The Al₂O₃+Si₃N₄ sample recorded an initial weight of 1.299 g and after the test it was 1.295 g, thus there was a wear loss of 0.004 g. Finally, the WC+Al₂O₃+Si₃N₄ sample registered a pre- test weight of 1.251 g and post-test weight of 1.249 g, and registered the minimum wear loss of 0.002 g. All this reveals that the WC+Al₂O₃+Si₃N₄

composite recorded the lowest wear loss and implies it is best when it comes to wear resistance as compared to the other two mixes. This analysis helps in understanding the wear behavior of the composite materials under specific conditions, aiding in the selection of materials for applications where wear resistance is crucial. The microstructural characterization of the developed composite samples was performed using optical microscopy analysis to evaluate the distribution, morphology, and homogeneity of the reinforcement phases within the matrix. Figure 7 represent the micrographs of two different composite specimens under identical magnifications. In the micrograph, the reinforcement particles are distributed uniformly and exhibit little agglomeration, indicating effective dispersion achieved during the fabrication process.

The interfacial interaction between the reinforcement and matrix looks to be acceptable, and the matrix appears dense, which is crucial for mechanical performance enhancement. Conversely,

the micrograph exhibits localized clustering of reinforcement phases with visible porosity regions, suggesting minor inconsistencies during processing. The presence of such clusters could potentially act as stress concentrators under mechanical loading, thereby influencing the overall mechanical properties adversely. Comparative analysis of these microstructures highlights the importance of processing parameters and mixing uniformity in achieving desired composite properties for high-performance applications. In a single pass of the FSP process, the aluminium metal matrix's reinforcing particle distribution considerably enhances the hardness and tensile properties. In Test Plate-1, which contains 50% WC and 50% Al₂O₃ particles, the hardness value is measured at 132 HV. In contrast, Test Plate-2 and Test Plate-3, which have different reinforcement combinations,

exhibit lower hardness values of 79 HV each. The maximum tensile strength was achieved in FSP Test Plate-1, which contains the 50% WC + 50% Al₂O₃ combination, with a tensile strength of 185 N/mm², followed by Test Plate-2 at 183 N/mm² and Test Plate-3 at 130 N/mm². During the wear analysis, it was found that the minimum wear rate occurred on Test Plate- 3, which contains the combination of WC + Al₂O₃ + Si₃N₄ reinforcement particles. This combination resulted in an extremely low wear rate, evaluated through the pin-on disc apparatus. Furthermore, microstructural investigations revealed that the surface composite layer on Test Plate-1, with its 50% WC and 50% Al₂O₃ reinforcement, is highly well-attached to the aluminum alloy substrate, demonstrating excellent adhesion.

Table 6. Weight of Testing Specimen before and After Wear.

Ratio	Before weight (g)	After weight (g)	Wear loss (g)
WC+Al ₂ O ₃	1.305	1.298	0.007
Al ₂ O ₃ +Si ₃ N ₄	1.299	1.295	0.004
WC+Al ₂ O ₃ +Si ₃ N ₄	1.251	1.249	0.002

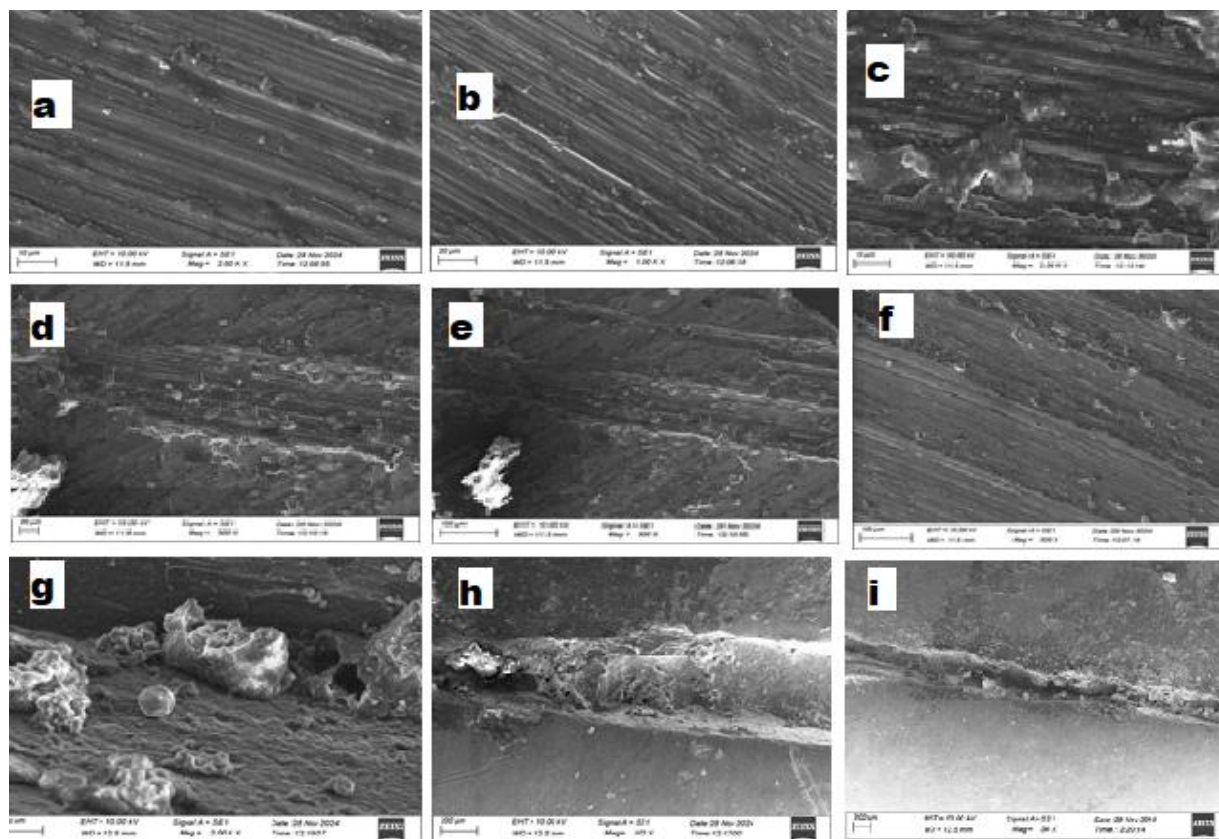


Figure 5. SEM Analysis of Test Plate 1- a, b, c, Test Plate-2 d, e, f and Test Plate 3- g, h, i.

The microstructural examination of the composite material was carried out using Scanning Electron Microscopy (SEM) to assess the wear surface characteristics after the wear testing process. Observation from Figure 5 reveals the presence of shallow wear tracks accompanied by minor micro-cracks, suggesting an abrasive wear mechanism dominated by surface ploughing and micro-cutting actions. The magnified images, particularly show discrete micro-pits and evidence of particle detachment, indicating localized delamination events during the wear process. Moreover, the grooved patterns and partial plastic deformation visible in the micrographs suggest that the composite experienced a combination of adhesive and abrasive wear modes. Further analysis emphasizes the severity of material removal at certain regions, where larger debris clusters and worn-out areas are distinctly visible. The accumulation of detached reinforcement particles and matrix fragments along the wear tracks implies repeated surface interaction, leading to progressive material degradation. The observed wear features suggest that although the reinforcement phases enhanced the overall wear resistance of the composite, certain zones were still susceptible to localized stress concentration, resulting in micro-crack initiation and propagation. These microstructural findings provide a deeper understanding of the wear mechanisms operating under the specific test conditions, reinforcing the significance of homogeneous reinforcement distribution and strong matrix-reinforcement bonding to improve the composite's wear performance. Figure 5 show the fractured surface of the material at different magnifications. The surface morphology reveals significant microstructural damage, characterized by the presence of voids, cracks, and roughness, indicating ductile fracture behavior. In the higher magnification image, localized plastic deformation and material tearing can be observed more clearly, along with some particle agglomeration on the surface. This suggests that during failure, the material underwent significant stretching before fracturing. The overall crack path appears more continuous and spread across a larger area. The irregularities and porosity along the crack propagation line highlight possible stress concentration zones and inter- granular failure. The presence of micro void coalescence points towards a classic ductile fracture mechanism, where voids nucleate, grow, and then merge, leading to ultimate material separation. Overall, the surface features indicate that the material has good toughness but failed under prolonged mechanical or environmental stress.

CONCLUSION

The fabrication of AA5083 with WC+Al₂O₃+Si₃N₄ (Tungsten Carbide, Aluminum Oxide, and Silicon Nitride) surface composites was successfully carried out using a single-pass FSP technique. This focused on various combinations of reinforcement particles

and analyzed their influence on the material's properties. Among the different surface composite configurations, the ratio-1 (50% WC and 50% Al₂O₃) exhibited significantly improved properties, including higher tensile strength and hardness, when compared to the other surface composites. This reinforced composite demonstrated exceptional performance of mechanical properties. The sample-1 composite displayed abnormal tensile strength, suggesting a notable improvement in material strength and stability. Furthermore, when subjected to wear analysis, the combined particles of WC and Al₂O₃ in the sample -1 composite were found to produce the lowest wear rate among all the tested samples. This indicates that surface composite's special blend of reinforcing particles successfully increased its resistance to wear, making it ideal for uses needing both durability and strength. The findings underscore the significant impact of the specific particle combination on the overall performance of AA5083 surface composites, especially in terms of mechanical strength and wear resistance.

REFERENCES

1. Patel, M., Jain, S. and Murugesan, J. (2024) Investigation of mechanical properties, fretting wear, and corrosion behaviour of AA6063/Si₃N₄ nanocomposites fabricated via friction stir processing. *Arabian Journal for Science and Engineering*, 1–11.
2. Almutairi, S. S., Mosleh, A. O., Mohamed, S. S., Mahmoud, T. S. and Moustafa, E. B. (2024) Max-phase Ti₃SiC₂ and diverse nanoparticle reinforcements for enhancement of the mechanical, dynamic, and microstructural properties of AA5083 aluminum alloy via FSP. *Nanotechnology Reviews*, **13**(1), 20240130.
3. Karmiris-Obratański, P., Papantoniou, I. G. and Leszczyńska-Madej, B. (2024) Microstructure, mechanical and tribological properties of AA5083-TiO₂ nanocomposite by multi-pass friction stir processing. *Archives of Civil and Mechanical Engineering*, **24**(4), 209.
4. Saravanakumar, S., Gopalakrishnan, S., Kalaiselvan, K. and Prakash, K. B. (2021) Microstructure and mechanical properties of Cu/RHA composites fabricated by friction stir processing. *Materials Today: Proceedings*, **45**, 879–883.
5. Yaknesh, S., Tharwan, M., Saminathan, R., Rajamurugu, N., Prakash, K. B., Ankit, Pasupathi, M. K., Sarojwal, A. and Gebreyohannes, D. T. (2022) Mechanical and microstructural investigation on AZ91B Mg alloys with tool tilt variation by friction stir welding. *Advances in Materials Science and Engineering*, **2022**(1), 8311413.

- 593 Saravanakumar, S., Satheesh Kumar, S., Chandrasekaran, M., Dadapeer, Doddamani., Mohammed Musthaq, M. S. and Prakash, K. B. Effect of Ceramic Reinforcement Chemistry on the Microstructure and Properties of Friction Stir Processed AA5083- Al₂O₃ & WC & Si₃N₄ Composites
6. Ghinous, R., Malki, M., Essadiqi, E. and Faqir, M. (2024) Versatile Applications of Friction Stir Techniques in Composite Hybridization Across Industries. In *Utilizing Friction Stir Techniques for Composite Hybridization*, IGI Global, 200-220.
 7. Arun, P. D., Annirut, P., Lokesh, K. A., Saketh, C. P., Vaira, V. R., Padmanaban, R. and Baghdad, A. (2023) Investigations on the texture and corrosion characteristics of AA5083 alloy reinforced with CeO₂ by friction stir processing. *Koroze a Ochrana Materiálu*, **67(1)**, 37–49.
 8. Saravanakumar, S., Prakash, K. B., Chandru, M. and Durairaj, M. (2016) Characterization of Copper Matrix Composite Reinforced with Aluminium Nitrate using Friction Stir Processing Techniques. *Iciems*, **1**, 58–62.
 9. Saravanakumar, S., Kalaiselvan, K., Prakash, K. B., Parkunam, M., Niranjan, S., Dharanish, N. and Akash, R. (2022) Mechanical behaviour and microstructure analysis of aluminium 2024 and 5052 using friction stir welding. *Materials Today: Proceedings*, **69**, 1437–1441.
 10. Mehdi, H., Mabuwa, S., Msomi, V. and Saxena, K. K. (2023) Influence of friction stir processing on the mechanical and microstructure characterization of single and double V-groove tungsten inert gas welded dissimilar aluminum joints. *Journal of Materials Engineering and Performance*, **32(17)**, 7858–7868.
 11. Bo, W. (2024) Fabrication of Metal Matrix Nanocomposite Surface on WE43 Using Friction Stir Processing for Biomedical Implant Application. *Doctoral Dissertation, University of Malaya, Malaysia*.
 12. Singhal, V., Shelly, D., Saxena, A., Gupta, R., Verma, V. K. and Jain, A. (2025) Study of the influence of nanoparticle reinforcement on the mechanical and tribological performance of aluminum matrix composites—A review. *Lubricants*, **13(2)**, 93.
 13. Soori, M. (2022) Mechanical Behavior of FSP process in the Aluminum Alloy 6061-5052 and 7075.
 14. Kurt, A., Uygur, I. and Cete, E. (2011) Surface modification of aluminium by friction stir processing. *Journal of Materials Processing Technology*, **211(3)**, 313–317.
 15. Arulmoni, V. J. and Mishra, R. S. (2014) Friction stir processing of aluminium alloys for defense applications. *International Journal of Advance Research and Innovation*, **2(2)**, 337–341.
 16. Kalashnikova, T., Chumaevskii, A., Kalashnikov, K., Knyazhev, E., Gurianov, D., Panfilov, A., Nikonov, S., Rubtsov, V. and Kolubaev, E. (2022) Regularities of friction stir processing hardening of aluminum alloy products made by wire-feed electron beam additive manufacturing. *Metals*, **12(2)**, 183.
 17. Golafshani, K. B., Nourouzi, S. and Jamshidi Aval, H. (2019) Evaluating the microstructure and mechanical properties of friction stir processed Al–Si alloy. *Materials Science and Technology*, **35(9)**, 1061–1070.
 18. Sanusi, K. O. and Akinlabi, E. T. (2017) Friction-stir processing of a composite aluminium alloy (AA 1050) reinforced with titanium carbide powder. *Mater. Tehnol.*, **51(3)**, 427–435.
 19. Mondal, M., Das, H., Hong, S. T., Jeong, B. S. and Han, H. N. (2019) Local enhancement of the material properties of aluminium sheets by a combination of additive manufacturing and friction stir processing. *CIRP Annals*, **68(1)**, 289–292.
 20. Zainelabdeen, I. H., Al-Badour, F. A., Suleiman, R. K., Adesina, A. Y., Merah, N. and Ghaith, F. A. (2022) Influence of friction stir surface processing on the corrosion resistance of Al 6061. *Materials*, **15(22)**, 8124.
 21. Joseph, G. B., Jeevahan, J., Saikiran, G. M. and Mageshwaran, G. (2016) Improving surface hardness of the aluminum plate by adding alumina powder by friction stir process. *International Journal of ChemTech Research*, **9(8)**, 587–593.
 22. Iwaszko, J. and Kudła, K. (2019) Effect of friction stir processing (FSP) on microstructure and hardness of AlMg10/SiC composite. *Bulletin of the Polish Academy of Sciences, Technical Sciences*, **67(2)**.
 23. Ma, Z. Y. (2008) Friction stir processing technology: a review. *Metallurgical and Materials Transactions A*, **39**, 642–658.
 24. Ma, Z. Y., Sharma, S. R. and Mishra, R. S. (2006) Effect of friction stir processing on the microstructure of cast A356 aluminum. *Materials Science and Engineering: A*, **433(1-2)**, 269–278.
 25. Sharma, V., Prakash, U. and Kumar, B. M. (2015) Surface composites by friction stir processing: A review. *Journal of Materials Processing Technology*, **224**, 117–134.
 26. Berbon, P. B., Bingel, W. H., Mishra, R. S., Bampton, C. C. and Mahoney, M. W. (2001) Friction stir processing: a tool to homogenize

- nanocomposite aluminum alloys. *Scripta Materialia*, **44(1)**, 61–66.
27. Kurt, A., Uygur, I. and Cete, E. (2011) Surface modification of aluminium by friction stir processing. *Journal of Materials Processing Technology*, **211(3)**, 313–317.
 28. Bauri, R., Yadav, D. and Suhas, G. (2011) Effect of friction stir processing (FSP) on microstructure and properties of Al–TiC in situ composite. *Materials Science and Engineering: A*, **528(13-14)**, 4732–4739.
 29. Wang, W., Han, P., Peng, P., Zhang, T., Liu, Q., Yuan, S. N., Huang, L. Y., Yu, H. L., Qiao, K. and Wang, K. S. (2020) Friction stir processing of magnesium alloys: a review. *Acta Metallurgica Sinica (English Letters)*, **33**, 43–57.
 30. Bharti, S., Ghetya, N. D. and Patel, K. M. (2021) A review on manufacturing the surface composites by friction stir processing. *Materials and Manufacturing Processes*, **36(2)**, 135–170.
 31. Yaknesh, S., Rajamurugu, N., Prakash, K. B., Saleel, C. A., Rajendran, P., Lee, I. and Arputharaj, B. S. (2024) A critical review on the performance and microstructural characteristics of materials fabricated through friction stir additive methods and deposition techniques. *Journal of Materials Research and Technology*.
 32. Saravanakumar, S., Prakash, K. B., Dinesh, D., Kumar, P. M., Fouad, Y., Soudagar, M. E. M., Ali, M. M. and Bashir, M. N. (2024) Optimizing friction stir processing parameters for aluminium alloy 2024 reinforced with SiC particles: A taguchi approach of investigation. *Journal of Materials Research and Technology*, **30**, 4847–4855.
 33. Hashmi, A. W., Mehdi, H., Mabuwa, S., Msomi, V. and Mohapatra, P. (2022) Influence of FSP parameters on wear and microstructural characterization of dissimilar TIG welded joints with Si-rich filler metal. *Silicon*, **14(17)**, 11131–11145.
 34. Ansari, A. J. and Anas, M. (2022) Review and analysis of the effect of variables on aluminium based surface composite fabricated through friction stir processing method. *International Journal of Advanced Technology and Engineering Exploration*, **9(95)**, 1552–1570.